Pergamon

Geochimica et Cosmochimica Acta, Vol. 67, No. 5, pp. 859–871, 2003

0016-7037/03 $30.00 + .00

doi:10.1016/S0016-7037(02)01227-9

# Natural realgar and amorphous AsS oxidation kinetics

MAGGY F. LENGKE[1,†] and REGINA N. TEMPEL[2,*]

[1]Graduate Program of Hydrologic Sciences, University of Nevada, Reno, Reno, Nevada 89557, USA
[2]Department of Geological Sciences, Mackay School of Mines, University of Nevada, Reno, Reno, Nevada 89557, USA

(*Received November* 16, 2001; *accepted in revised form September* 19, 2002)

**Abstract**—The oxidation rates of natural realgar and amorphous synthetic AsS by dissolved oxygen were evaluated using mixed flow reactors at pH 7.2 to 8.8 and dissolved oxygen contents of 5.9 to 16.5 ppm over a temperature range of 25 to 40°C. The ratios of As/S are stoichiometric for all amorphous AsS oxidation experiments except for two experiments conducted at pH ~8.8. In these experiments, stoichiometric ratios of As/S were only observed in the early stages of AsS (am) oxidation whereas lower As/S ratios were observed during steady state. For realgar oxidation experiments, the As/S ratio is less than the stoichiometric ratio of realgar, ranging between 0.61 and 0.71. This nonstoichiometric release of As and S to solution indicates that realgar oxidation is more selective for S after the rates of oxidation become constant. All measured oxidation rates at 25°C can be described within experimental uncertainties as follows:

| Rate Expression | Activation Energy (kJ/mol) |
|---|---|
| $R_{(Realgar/As)} = 10^{-9.63(\pm0.41)}[DO]^{0.51(\pm0.08)}[H^+]^{-0.28(\pm0.05)}$ | 64.2 ± 9.8 |
| $R_{(Realgar/S)} = 10^{-9.74(\pm0.35)}[DO]^{0.54(\pm0.05)}[H^+]^{-0.31(\pm0.04)}$ | 62.2 ± 9.0 |
| $R_{(AsS(am))} = 10^{-13.65(\pm0.82)}[DO]^{0.92(\pm0.08)}[H^+]^{-1.09(\pm0.10)}$ | 124 ± 18.8 |

where R signifies the steady-state oxidation rate (mol $m^{-2}s^{-1}$), [DO] is dissolved oxygen concentration (M), and $[H^+]$ is the proton concentration (M). Arsenic (III) and As(V) are both present in solution, and As(III) is the dominant species in most experiments. Intermediate sulfur species besides sulfate, sulfite, and thiosulfate are the important products during realgar and AsS (am) oxidation.

Comparison of realgar and AsS (am) oxidation rates shows that at similar conditions, the rates of AsS (am) are always faster by about a factor ranging from 2 to 38. The oxidation of realgar involves breaking bonds in the realgar crystal, whereas AsS (am) oxidation does not include crystallographic framework destruction due to the amorphous nature of the solid. *Copyright © 2003 Elsevier Science Ltd*

## 1. INTRODUCTION

High arsenic concentrations occur in the United States and in other parts of the world such as in Bangladesh, India, Taiwan, Argentina, China, and Mexico (Welch et al., 1988; Smith et al., 1992). Many arsenic investigations are focused mainly on the removal of arsenic from natural waters, and only a limited number of studies have looked into the processes that release arsenic from weathered solids or minerals such as realgar, orpiment, and arsenopyrite.

In weathering processes, reaction kinetics are often the controlling factors in deciding fate and transport of the elements. In this study, realgar and amorphous AsS [AsS (am)] are chosen for study because arsenic (II) sulfide solid phases provide models for studying the kinetics of weathering processes of other, more chemically diverse arsenic sulfide solids. Arsenic (II) sulfide solids are good models because the crystalline structure and amorphous forms of AsS are known (Forneris, 1969).

AsS (am) is found on the carbonate-hosted Lengenbach Pb-Zn-As-Tl-Ba mineral deposits in Switzerland (Hugi, 1988), and realgar is one of the most common arsenic minerals found in hydrothermal deposits. In Carlin-type gold deposits, the gold occurs as discrete grains and as solid-solution in realgar (Radtke, 1981). The association of realgar and gold makes the study of realgar oxidation valuable for the mining industry, including the recovery of precious metals from realgar ores through hydrometallurgy. Thus, an understanding of the oxidative dissolution behavior of realgar and amorphous or glass realgar composition provides insight to arsenic sulfide oxidation reactions in general.

Numerous studies have focused on arsenopyrite oxidation, and a few studies (Ehrlich, 1963; Lazaro et al., 1997; Lengke and Tempel, 2001, 2002) have investigated natural orpiment or $As_2S_3$ (am) oxidation. Only one study has described realgar oxidation, an experimental study conducted by Lazaro et al. (1997) utilizing an electrochemical method in acidic medium. The oxidation reactions proposed by Lazaro et al. (1997) involve two steps as follows:

* Author to whom correspondence should be addressed (gina@mines.unr.edu).
† Present address: University of Western Ontario, London, Ontario N6A 5B7, Canada

$$As_2S_2 + 14H_2O \rightarrow 2H_3AsO_3 + 2HSO_4^- + 20H^+ + 18e^- \quad (1)$$

$$H_3AsO_3 + H_2O \rightarrow H_3AsO_4 + 2H^+ + 2e^- \quad (2)$$

The reaction rates and activation energies were not determined in that study.

The main goal of our research has been to determine the oxidation rates of arsenic sulfide solids (Lengke, 2001). In this paper, we discuss the rate expressions for realgar and AsS (am) oxidation. Dissolved oxygen, pH, and temperature were evaluated to determine the dependence factors of these parameters on the oxidation rates. The differences in oxidation behavior of synthetic glass vs. realgar are also compared and discussed.

## 2. MATERIAL AND METHODS

### 2.1. Characterization and Pretreatment of the Solid

Synthetic AsS (am) (91.7% metal purity) obtained from Alfa Aesar Co., Ward Hill, Massachusetts, USA was used in this study. The composition of AsS (am) is 48.3 atomic % of As and 51.7 atomic % of S ($As_{0.48}S_{0.52}$). The starting material was rinsed with ethanol several times in an ultrasonic bath until a clear supernatant solution was obtained. Then, the samples were wet sieved to obtain a size fraction of 44 to 125 $\mu$m, dried, and stored in a vacuum desiccator.

Natural realgar samples from the Getchell Mine, Golconda, Nevada were used in oxidation experiments in this study. The mineral composition of natural realgar based on bulk chemical analysis for As and S is $As_{0.49}S_{0.51}$. Initially the realgar samples were hand picked to separate them from other sulfide and nonsulfide phases (mostly orpiment with small amounts of silicate, carbonate, and sulfide minerals), and were crushed and sieved into a size fraction between 44 and 125 $\mu$m. The realgar sample was then soaked overnight in hydrochloric acid 0.01 mol/L, washed in distilled water, and dried. To remove fines, the realgar powder was washed with ethanol in an ultrasonic bath and the cleaning procedure was repeated until the supernatant was clear. The realgar powder samples were then dried at room temperature and stored in a vacuum desiccator until use.

Trace metals in both cleaned bulk realgar and AsS (am) were determined by aqua regia extraction ($HNO_3$/HCl) and inductively coupled plasma mass spectrometry (ICP-MS). Two bulk samples for each solid were analyzed, and these results were then averaged, as shown in Table 1. Both realgar and AsS (am) samples contain significant amounts of antimony (Sb) and mercury (Hg) relative to other trace metals. In addition, the synthetic AsS (am) is relatively enriched in lead (Pb), nickel (Ni), selenium (Se), bismuth (Bi), and chromium (Cr).

X-ray diffraction (XRD) analysis of the material before and after experiments was conducted using Philips x-ray generator (XRG) 3100 X-ray diffractometer with $CuK_\alpha$ radiation generated at 40 kV and 30 mA. The XRD pattern of AsS (am) shows a broad peak centered around 18° and 34° (2-theta), and XRD of the realgar sample confirmed the removal of orpiment, carbonate, and silicate minerals. Some unidentified peaks were also observed. The presence of feldspars was detected by scanning electron microscopy/energy-dispersive spectroscopy (SEM/EDS). However, no further attempt to remove feldspars was made because they are only present in minor amounts and further pretreatment steps may cause alteration of the realgar surface. The surfaces of fresh/cleaned and oxidized realgar and AsS (am) powder coated with gold were studied using a JEOL JSM-840A scanning electron microscope. The specific surface area of the fresh/cleaned and oxidized realgar and AsS (am) powder was determined by Kr adsorption using the multipoint Brunauer, Emmet, and Teller method (BET) (Brunauer et al., 1938). The uncertainty on BET surface area measurements is ±6% or 8% for AsS (am) and realgar, respectively.

### 2.2. Experimental Methodology and Solution Analyses

All oxidation experiments were performed in a 450-mL mixed flow reactor that is described in detail by Lengke and Tempel (2001). The influence of dissolved oxygen on the realgar and AsS (am) oxidation was studied by varying dissolved oxygen in the feed solution with either highly pure oxygen (99.9%) or ambient air. Feed solutions of pH 7 to 9 were prepared with analytical reagent grade sodium carbonate ($Na_2CO_3$) and/or sodium bicarbonate ($NaHCO_3$) in distillated, deionized water. Ionic strength of the feed solutions was fixed to 0.01 mol/L using sodium chloride (NaCl).

The outlet solution, pH, DO, and Eh were also continuously monitored. The pH/Eh and DO values of all solutions were measured using an Orion 420A pH/millivolt-meter and an Orion 862A DO-meter. The analytical uncertainties in pH and DO measurements are ±0.02 pH unit and ±0.05 ppm. The reactor was wrapped with aluminum foil for all experiments to avoid further oxidation by ultraviolet light. Achievement of steady-state conditions was verified with a minimum of six constant total As and S concentrations that are less than 6% standard deviation.

Total As and S concentrations were analyzed with inductively coupled plasma atomic emission spectroscopy (ICP-AES) by Acme Analytical Laboratory, Vancouver, Canada. The uncertainty in measured As and S in the test solutions is ≤5% with the detection limits of 30 ppb (0.0004 mM) and 0.1 ppm (0.003 mM) for As and S, respectively.

Sulfate ($SO_4^{2-}$), sulfite ($SO_3^{2-}$), and thiosulfate ($S_2O_3^{2-}$) were determined using a Dionex EX100 Ion Chromatograph (IC) by Huffman Analytical Laboratory, Golden, Colorado. The samples were preserved using 0.1 mol/L triethanolamine for sulfite and frozen until analysis, approximately a week. Analytical detection limits were 0.1 ppm for $SO_4^{2-}$ and 0.3 ppm for $SO_3^{2-}$ and $S_2O_3^{2-}$ with uncertainties of ±0.1 ppm for $SO_4^{2-}$ and ±0.3 ppm for $SO_3^{2-}$ and $S_2O_3^{2-}$.

Arsenic (III) was determined using hydride generation coupled with a Varian Spectra 220 atomic absorption spectrometer (AA). The output solutions for arsenic species were stored in amber polyethylene bottles and were frozen until analysis without chemical preservative, approximately within a week. The uncertainty in measured As(III) is ±5%. As(V) was calculated by subtracting the As (III) from total As measured using ICP-AES from the same solution.

Table 1. Chemical composition of realgar and AsS (am).

| Element | Units | Realgar | AsS (am) |
|---|---|---|---|
| Sb | ppm | 4854.75 | 1520.91 |
| Hg | ppm | >100.00 | >100.00 |
| Se | ppm | 69.65 | 166.10 |
| Cr | ppm | 50.15 | 196.65 |
| Zn | ppm | 28.15 | 44.20 |
| Te | ppm | 17.12 | 11.11 |
| Ni | ppm | 17.05 | 123.75 |
| V | ppm | 14.50 | <2.00 |
| Cu | ppm | 11.80 | 36.92 |
| Tl | ppm | 8.47 | 3.93 |
| Mo | ppm | 5.43 | 10.62 |
| Sr | ppm | 1.90 | 2.55 |
| W | ppm | 0.30 | 0.30 |
| Cd | ppm | 0.23 | 3.42 |
| Ga | ppm | 0.25 | 0.15 |
| U | ppm | 0.20 | <0.10 |
| Sc | ppm | 0.20 | 1.50 |
| Pb | ppm | 0.08 | 230.99 |
| Bi | ppm | 0.04 | 89.04 |
| Mn | ppm | <1.00 | <1.00 |
| La | ppm | <0.50 | <0.50 |
| Ba | ppm | <0.50 | 3.60 |
| Co | ppm | <0.10 | 15.10 |
| Th | ppm | <0.10 | <0.10 |
| Ag | ppb | 807.50 | 313.50 |
| Au | ppb | 428.05 | 16.20 |
| Ca | % | 0.58 | 0.04 |
| Fe | % | 0.06 | 0.25 |
| Al | % | 0.02 | 0.01 |

Table 2. Experimentally measured realgar oxidation rates. Initial surface area of realgar is 0.76 $m^2/g$. Final Sa is the surface area of oxidized realgar.

| | | | | | Input | | | Steady state | | | | | | | | | | |
|---|---|---|---|---|---|---|---|---|---|---|---|---|---|---|---|---|---|---|
| Exp. # | Flow rate (mL/min) | Temp (C) | Mass (g) | Time (min) | pH | DO (ppm) | Eh (V) | pH | DO (ppm) | Eh (V) | mAs (mM) | mS (mM) | As/S | Final Sa ($m^2g^{-1}$) | Steady state $R_{As}$ (mol $m^{-2}$ $s^{-1}$) | Steady state $R_S$ (mol $m^{-2}$ $s^{-1}$) | Error $R_{As}$ (%) | Error $R_S$ (%) |
| Z | 10.03 | 25 | 4.948 | 1735 | 7.91 | 7.08 | 0.290 | 8.02 | 6.53 | 0.132 | 0.018 | 0.027 | 0.67 | 1.22 | 5.10E-10 | 7.57E-10 | 6 | 5 |
| ZZZ | 10.03 | 25 | 4.948 | 1735 | 8.00 | 7.00 | 0.290 | 8.01 | 6.47 | 0.131 | 0.016 | 0.024 | 0.67 | 1.22 | 4.45E-10 | 6.63E-10 | 6 | 5 |
| Y | 10.03 | 30 | 5.189 | 1725 | 7.98 | 6.37 | 0.347 | 8.00 | 5.33 | 0.141 | 0.016 | 0.024 | 0.68 | 0.61 | 8.53E-10 | 1.25E-09 | 6 | 5 |
| ZZ | 10.03 | 30 | 5.042 | 1710 | 8.02 | 6.37 | 0.297 | 8.04 | 5.75 | 0.098 | 0.018 | 0.028 | 0.64 | 0.95 | 6.25E-10 | 9.77E-10 | 6 | 5 |
| X | 10.03 | 40 | 5.174 | 1745 | 8.00 | 5.33 | 0.323 | 8.13 | 3.94 | 0.095 | 0.030 | 0.044 | 0.68 | 0.79 | 1.21E-09 | 1.78E-09 | 6 | 5 |
| YY | 10.03 | 40 | 5.031 | 1710 | 8.00 | 5.44 | 0.246 | 7.73 | 3.58 | 0.063 | 0.034 | 0.047 | 0.71 | 0.79 | 1.41E-09 | 1.98E-09 | 6 | 5 |
| W | 10.03 | 25 | 5.265 | 1720 | 7.18 | 7.08 | 0.311 | 8.68 | 6.06 | 0.120 | 0.018 | 0.028 | 0.64 | 0.93 | 6.13E-10 | 9.58E-10 | 6 | 5 |
| WW | 10.03 | 25 | 5.061 | 1710 | 7.26 | 7.00 | 0.301 | 7.80 | 6.29 | 0.107 | 0.011 | 0.017 | 0.67 | 1.03 | 3.55E-10 | 5.27E-10 | 6 | 5 |
| WWW | 10.03 | 25 | 5.265 | 3160 | 7.17 | 7.00 | 0.311 | 8.74 | 6.05 | 0.116 | 0.018 | 0.028 | 0.64 | 0.90 | 6.33E-10 | 9.92E-10 | 6 | 5 |
| V | 10.03 | 25 | 5.003 | 1655 | 8.06 | 18.00 | 0.295 | 8.00 | 16.54 | 0.166 | 0.017 | 0.026 | 0.68 | 0.75 | 7.81E-10 | 1.14E-09 | 6 | 5 |
| XX | 10.03 | 25 | 5.002 | 1715 | 8.05 | 18.00 | 0.289 | 8.02 | 15.57 | 0.120 | 0.029 | 0.047 | 0.62 | 1.49 | 6.54E-10 | 1.05E-09 | 6 | 5 |
| U | 10.03 | 25 | 5.099 | 1740 | 8.00 | 18.50 | 0.271 | 8.05 | 16.29 | 0.156 | 0.018 | 0.028 | 0.65 | 0.79 | 7.62E-10 | 1.17E-09 | 6 | 5 |
| S | 10.03 | 25 | 5.152 | 1715 | 8.06 | 15.00 | 0.289 | 8.02 | 13.42 | 0.172 | 0.014 | 0.023 | 0.62 | 0.79 | 5.93E-10 | 9.62E-10 | 6 | 5 |
| T | 10.03 | 25 | 5.089 | 1725 | 8.91 | 7.01 | 0.260 | 8.80 | 6.10 | 0.103 | 0.018 | 0.028 | 0.67 | 0.75 | 8.00E-10 | 1.20E-09 | 6 | 5 |
| UU | 10.03 | 25 | 5.059 | 1715 | 8.88 | 7.01 | 0.271 | 8.78 | 6.32 | 0.087 | 0.013 | 0.021 | 0.61 | 0.75 | 5.72E-10 | 9.39E-10 | 6 | 5 |
| VV | 10.03 | 25 | 5.076 | 1720 | 7.90 | 7.00 | 0.303 | 8.40 | 6.40 | 0.127 | 0.015 | 0.023 | 0.65 | 0.99 | 5.02E-10 | 7.78E-10 | 6 | 5 |
| P | 10.03 | 25 | 5.022 | 1715 | 7.93 | 7.08 | 0.261 | 8.10 | 5.87 | 0.104 | 0.015 | 0.022 | 0.65 | 1.23 | 3.98E-10 | 6.08E-10 | 6 | 5 |

### 2.3. Calculations

Steady-state oxidation rates, R (mol $m^{-2}$ $s^{-1}$), in a mixed flow reactor were computed using the following equation (Levenspiel, 1972):

$$R = \frac{q}{A}(C) \tag{3}$$

where C is the output solution concentration (M), q is the flow rate through the system (L $s^{-1}$), and A is the total surface area of solid ($m^2$).

The error ($\varepsilon$) associated with the calculated rates (R) was estimated using the error propagation method (Barrante, 1998) by the following equation:

$$(\varepsilon(R))^2 = \left(\frac{C}{A}\right)^2(\varepsilon(q))^2 + \left(\frac{q \cdot C}{A^2}\right)^2(\varepsilon(A))^2 + \left(\frac{q}{A}\right)^2(\varepsilon(C))^2 \tag{4}$$

Uncertainties considered above come from the measurements of solution concentration (C) flow rate (q), and mineral or solid surface area (A).

## 3. RESULTS AND DISCUSSION

The results and conditions of experiments are compiled in Tables 2 and 3. The duration of most experiments was ~30 h and steady-state conditions were reached after 20 h. However, longer experiments for both realgar and AsS (am) oxidation were also conducted. Two experiments of AsS (am) oxidation at lower pH values (pH 7.2) were conducted for a longer duration (60 h) to achieve the stoichiometric ratio for AsS (am) in solution. Initial rates of realgar and AsS (am) oxidation are often much greater than the rates after 5 h and poorly reproduced in replicate experiments (Figs. 1 and 2). These initial, time-dependent rates may be the result of preferential dissolu-

Table 3. Experimentally measured AsS (am) oxidation rates. Initial surface area of AsS (am) is 0.29 $m^2/g$. Final Sa is the surface area of oxidized AsS (am).

| | | | | | Input | | | Steady state | | | | | | | | | | |
|---|---|---|---|---|---|---|---|---|---|---|---|---|---|---|---|---|---|---|
| Exp. # | Flow rate (mL/min) | Temp (C) | Mass (g) | Time (min) | pH | DO (ppm) | Eh (V) | pH | DO (ppm) | Eh (V) | mAs (mM) | mS (mM) | As/S | Final Sa ($m^2g^{-1}$) | Steady state $R_{As}$ (mol $m^{-2}s^{-1}$) | Steady state $R_S$ (mol $m^{-2}s^{-1}$) | Error $R_{As}$ (%) | Error $R_S$ (%) |
| A | 10.03 | 25 | 5.072 | 1750 | 8.91 | 7.00 | 0.278 | 8.76 | 6.59 | 0.034 | 0.140 | 0.214 | 0.66 | 0.23 | 2.01E-08 | 3.06E-08 | 6 | 3 |
| AA | 10.03 | 25 | 5.013 | 1705 | 8.92 | 7.00 | 0.249 | 8.64 | 6.58 | 0.035 | 0.160 | 0.250 | 0.64 | 0.23 | 2.32E-08 | 3.63E-08 | 6 | 3 |
| B1 | 10.03 | 25 | 5.080 | 3645 | 7.40 | 7.00 | 0.303 | 7.21 | 6.82 | 0.110 | 0.007 | 0.006 | 1.08 | 0.25 | 8.90E-10 | 8.25E-10 | 6 | 5 |
| B2 | 10.03 | 25 | 5.060 | 3240 | 7.45 | 7.00 | 0.306 | 7.21 | 6.84 | 0.112 | 0.007 | 0.006 | 1.08 | 0.25 | 8.93E-10 | 8.28E-10 | 6 | 5 |
| C | 10.03 | 25 | 5.080 | 1715 | 7.90 | 7.00 | 0.267 | 7.89 | 6.80 | 0.082 | 0.019 | 0.022 | 0.89 | 0.28 | 2.31E-09 | 2.61E-09 | 6 | 4 |
| CC | 10.03 | 25 | 5.080 | 1715 | 7.90 | 7.00 | 0.267 | 7.87 | 6.77 | 0.082 | 0.019 | 0.021 | 0.91 | 0.28 | 2.28E-09 | 2.51E-09 | 6 | 5 |
| D | 10.03 | 30 | 5.031 | 1710 | 7.92 | 6.37 | 0.248 | 7.82 | 6.18 | 0.087 | 0.019 | 0.022 | 0.86 | 0.30 | 2.06E-09 | 2.40E-09 | 6 | 4 |
| DD | 10.03 | 30 | 5.031 | 1710 | 7.92 | 6.37 | 0.248 | 7.82 | 6.15 | 0.088 | 0.019 | 0.023 | 0.82 | 0.30 | 2.14E-09 | 2.60E-09 | 6 | 4 |
| E | 10.03 | 40 | 5.082 | 1690 | 7.92 | 5.44 | 0.227 | 7.59 | 5.11 | 0.066 | 0.066 | 0.073 | 0.90 | 0.25 | 8.65E-09 | 9.59E-09 | 6 | 5 |
| EE | 10.03 | 40 | 5.080 | 1690 | 7.92 | 5.44 | 0.227 | 7.56 | 5.10 | 0.071 | 0.068 | 0.072 | 0.94 | 0.25 | 8.83E-09 | 9.43E-09 | 6 | 5 |
| F | 10.03 | 25 | 5.060 | 1715 | 8.04 | 16.95 | 0.305 | 7.73 | 15.81 | 0.094 | 0.050 | 0.047 | 1.05 | 0.28 | 5.96E-09 | 5.65E-09 | 6 | 5 |
| FF | 10.03 | 25 | 5.082 | 1715 | 8.04 | 13.50 | 0.305 | 7.93 | 12.79 | 0.108 | 0.030 | 0.035 | 0.86 | 0.23 | 4.20E-09 | 4.88E-09 | 6 | 4 |
| H | 10.03 | 25 | 5.075 | 1725 | 8.10 | 13.26 | 0.275 | 8.01 | 12.93 | 0.100 | 0.030 | 0.031 | 0.96 | 0.24 | 4.12E-09 | 4.27E-09 | 6 | 5 |

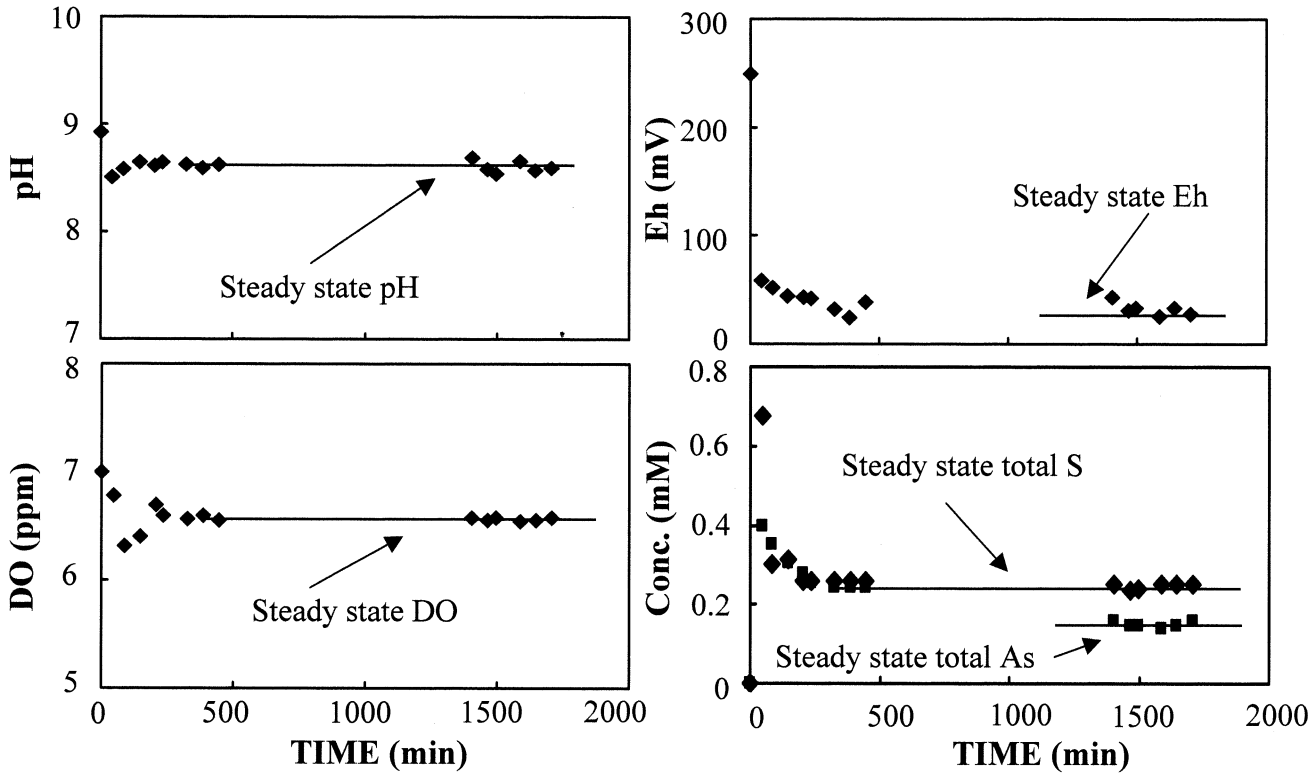


Fig. 1. Evolution of pH, DO, Eh, As, and S concentrations during AsS (am) oxidation until steady-state conditions are achieved (Exp. # AA).

tion of fine particles at strained sites, cracks, or other structural distortions. After approximately 20 h, oxidation rates for most experiments become reproducible and remain constant for up to 30 h. The specific surface areas of the oxidized realgar and AsS (am) grains were essentially similar to those of unreacted grains, and the oxidation rates were normalized to final surface area. The rates of realgar and AsS (am) oxidation are reproduced in replicate experiments. The dissolved mass that was calculated based on the output concentrations of total As and S, was less than 2% or 9% of the starting material throughout the experiments for realgar and AsS (am), respectively.

The estimated uncertainties of the oxidation rates were assessed using the error propagation equation above (Eqn. 4). The estimated errors are the sum of the uncertainties associated with the measurement of solution compositions, fluid flow rates, and surface area. These uncertainties were determined by analyzing the same sample three times. Uncertainties in the measured values of the total As and S at steady-state conditions are $\leq$5%. Uncertainties in fluid flow rate measurements are small ($\leq$1%). Uncertainties in repeated BET surface area measurements are $\pm$6% or 8% for AsS (am) and realgar, respectively. Thus, the errors among AsS (am) and realgar oxidation rates are $<$10% and are mostly derived from the BET surface area measurements.

### 3.1. Stoichiometry

For most AsS (am) oxidation experiments, the ratios of total As to total S concentrations in the output solution during steady-state conditions are very close to the stoichiometric ratio ($\sim$0.93), ranging from 0.82 to 1.05, except for experiments conducted at pH $\sim$8.8 (Table 3, Exp. # A and AA). In these higher pH experiments, oxidation of AsS (am) is stoichiometric at the beginning stage and becomes less stoichiometric at steady-state conditions where the final As/S ratio is $\sim$0.64 to 0.66. Total As and S releases at pH $\sim$8.8 were reproduced in duplicate experiments (Table 3, Exp. # A and AA). Although the stoichiometric ratio was not achieved, total S release was always constant after $\sim$3 h until the end of experiments. Conversely, total As release was still decreasing with time after 3 h and reached a constant value after 20 h (Fig. 1). For experiments at pH 7.2, the stoichiometric value was reached in a longer period (after 35 h), as shown in Figure 3. While total S release was constant after 20 h, total As release was still declining. A constant value for total As release was achieved after 30 h. Due to the more rapid approach to constant values, only total S release was used to determine the dependency factors of AsS (am) oxidation upon DO, pH, and temperature.

For all experiments, oxidation of realgar appeared far from stoichiometric at the early stages, and became close to stoichiometric with time (Fig. 2). For all experiments, the As/S ratio ranges between 0.61 to 0.71 at steady-state conditions (Table 2). This ratio is lower than the stoichiometric ratio of As and S in realgar which is $\sim$0.96. For all experiments, the initial release rates of As were faster than those for S. This early preferential release of As is consistent with the fact that As-As bonds are weaker than As-S bonds (Douglass et al., 1992).

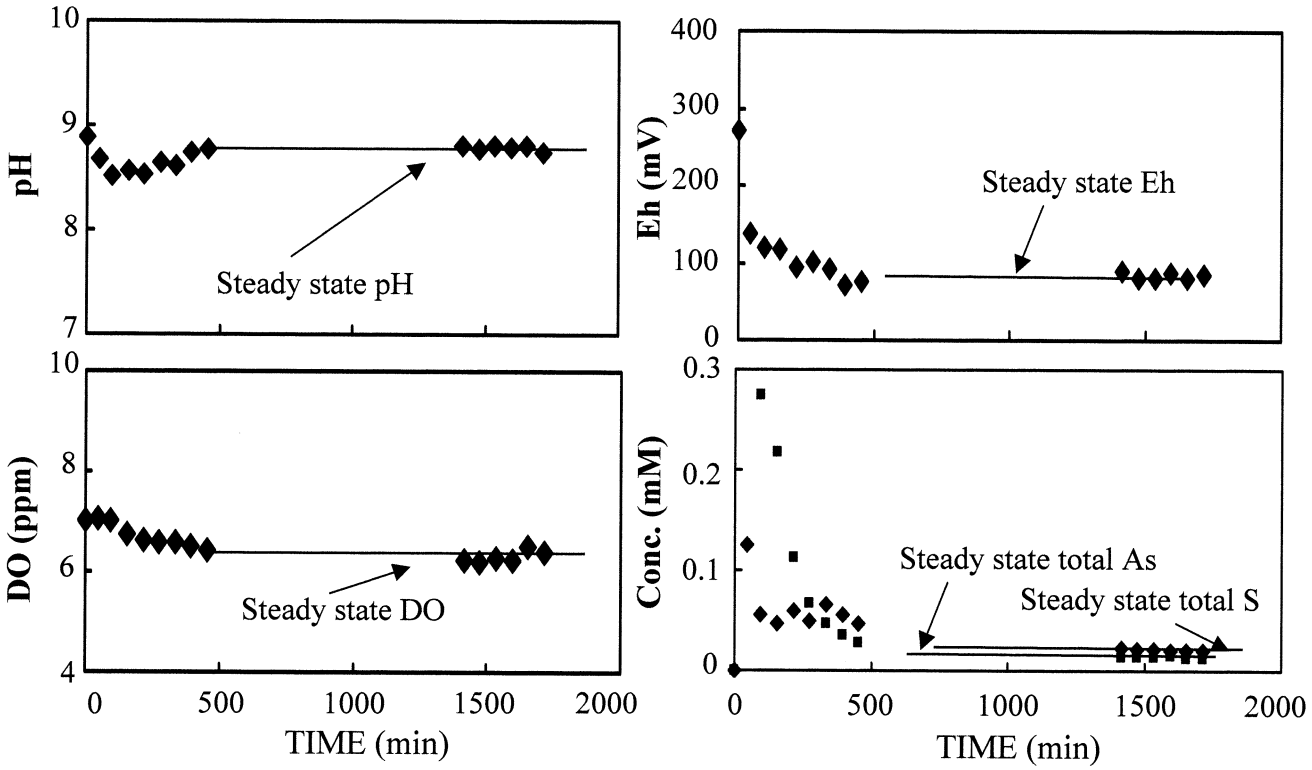


Fig. 2. Variation of As, S, pH, DO, and Eh as a function of time during realgar oxidation (Exp. # UU).

Moreover, a study conducted on the surface oxidation of arsenopyrite showed that As is readily oxidized species while sulfur is more slowly oxidized during reaction with air-saturated distilled water (Nesbitt et al., 1995). Also, $As^{3+}$ may diffuse out of the mineral lattice more readily to maintain charge balance after the partial oxidation of $As^{2+}$ and $S^{2-}$ within the lattice during an early step of oxidation.

During steady-state conditions in our experiments, the release of S was always slightly faster than the release of As over the entire pH, DO, and temperature range. This difference in release rates may be due to a lower rate of diffusion of As from lattice realgar to oxidized surfaces after rapid As leaching during the initial stages of oxidation. Additionally, a previous study has shown that cation diffusion rates are low during surface oxidation of pyrite, so cation release is likely limited to the near surface region of the mineral (Buckley and Woods, 1987). These factors may explain the differences in release rates of As and S over the duration of the experiments.

Nonstoichiometric or incongruent dissolution commonly has been attributed to the precipitation of secondary phases (Rimstidt et al., 1994; Nicholson and Scharer, 1994). In this study, XRD analysis of both oxidized realgar and AsS (am) samples yielded the same results as fresh/unoxidized realgar samples. No secondary phases were observed in the oxidized realgar samples using SEM, although this method may not be sensitive enough to detect precipitates unless they are widely spread across the mineral surfaces. However, SEM photomicrographs of some AsS (am) grains (Table 3, Exp. # A and AA) revealed the minor presence of many fine particles on AsS (am) surfaces (Fig. 4). Similar particles were also observed by Douglass et al. (1992) on realgar surfaces during alteration of realgar to pararealgar by light and Douglass et al. (1992) concluded that these particles were formed as a precursor for pararealgar formation with a composition similar to realgar. In this study, the composition of these particles could not be accurately determined using SEM/EDS because of the flocculent and porous nature of this phase, and only the spectra of As and S were observed using SEM/EDS. Moreover, SEM is not a surface-sensitive technique. Further surface analysis of oxidized grains is necessary to determine the composition of secondary phases that may be responsible for As loss from solution.

Solubility calculations using the geochemical code PHREEQC (Parkhurst, 1995) show that the experimental solutions were undersaturated with respect to theoretical secondary phases (arsenolite ($As_4O_6$), claudetite ($As_4O_6$), orpiment ($As_2S_3$), sulfur (S), mirabilite ($Na_2SO_4 0.10H_2O$), thenardite ($Na_2SO_4$), and $As_2O_5$) during the course of the experiments. Thermodynamic data for other As-bearing minerals are not available, and it is not likely that these minerals would be present at the considered pH and As concentrations of our experiments.

Dissolution of trace constituents or impurities within the solid could also account for the observed nonstoichiometric dissolution. Evidence of nonstoichiometric dissolution due to compositional variation was not observed in SEM photomicrographs, but it may occur on a scale too small to be detected. Although the samples were hand-picked and carefully cleaned during preparation, other sulfide minerals may be present as secondary replacements or compositional or structural adjustments in the form of exsolution (Craig and Vaughan, 1981).

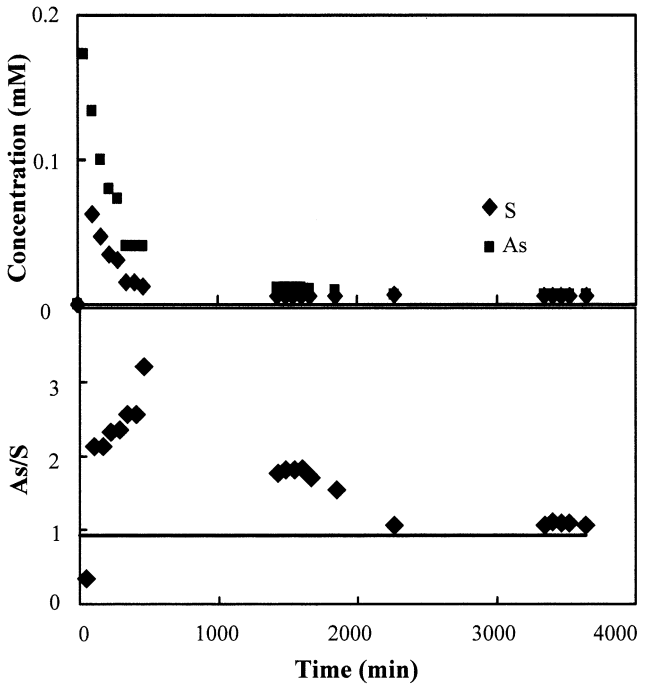


Fig. 3. Total As and S concentrations and ratio of As/S during AsS (am) oxidation (Exp. # B1).

Thus, other sulfide minerals such as orpiment, cinnabar, stibnite, chalcopyrite, and sphalerite may also be present in minor amounts within realgar because the bulk chemical analysis of realgar shows relatively significant amounts of mercury (Hg), antimony (Sb), copper (Cu), iron (Fe), and zinc (Zn) (Table 1). These impurity minerals may further contribute to the observed chemistry of outlet solutions.

### 3.2. The Effect of Variable Dissolved Oxygen Concentrations and pH

Only total S release during steady state of AsS (am) oxidation was used to determine the effect of DO, pH, and temperature on AsS (am) oxidation. Due to the nonstoichiometric ratio of As/S for realgar oxidation, it becomes uncertain which single element should represent the oxidation rates. Therefore, both total As and S release rates from realgar oxidation were used to determine the effect of pH and DO on the oxidation rates.

The oxidation rates of both realgar and AsS (am) increase with increasing pH and DO concentrations. The rate dependence on dissolved oxygen was assessed by varying dissolved oxygen concentration from 5.9 to 16.5 ppm or 6.8 to 15.8 ppm at 25°C and pH ~8 for realgar and AsS (am), respectively. The plot of log realgar oxidation rate vs. log dissolved oxygen yields slopes of 0.51 ± 0.08 and 0.54 ± 0.05 for As and S, respectively (Table 2, Exp. # P, S, U, V, XX, Z, and ZZZ; Fig. 5). The reaction order for AsS (am) derived from the plot as the slope of the lines is 0.92 ± 0.08 (Table 3, Exp. # C, CC, F, FF, and H; Fig. 5). This indicates that the dissolved oxygen content significantly influences the rate of realgar and AsS (am) oxidation.

The effect of pH was investigated within the pH range of 7.2 to 8.8 or 7.8 to 8.8 at 25°C for AsS (am) and realgar, respectively. The plot of (log rate-n log DO) vs. pH yields slopes of 1.09 ± 0.10 for AsS (am), as shown in Figure 6 (Table 3, Exp. # A, AA, C, CC, B1, and B2). The dependence factors of pH on the realgar oxidation are 0.28 ± 0.05 and 0.31 ± 0.04, as shown in Figure 6 (Table 2, Exp. # T, UU, VV, W, WW, Z, and ZZZ). These results indicate that the rates of realgar and AsS (am) oxidation are affected by pH. Although the oxidation rates of realgar are nonstoichiometric, the reaction order of pH and DO are similar based on concentrations of As and S. The dependence of realgar and AsS (am) oxidation rates (R) on proton and DO concentrations is as follows:

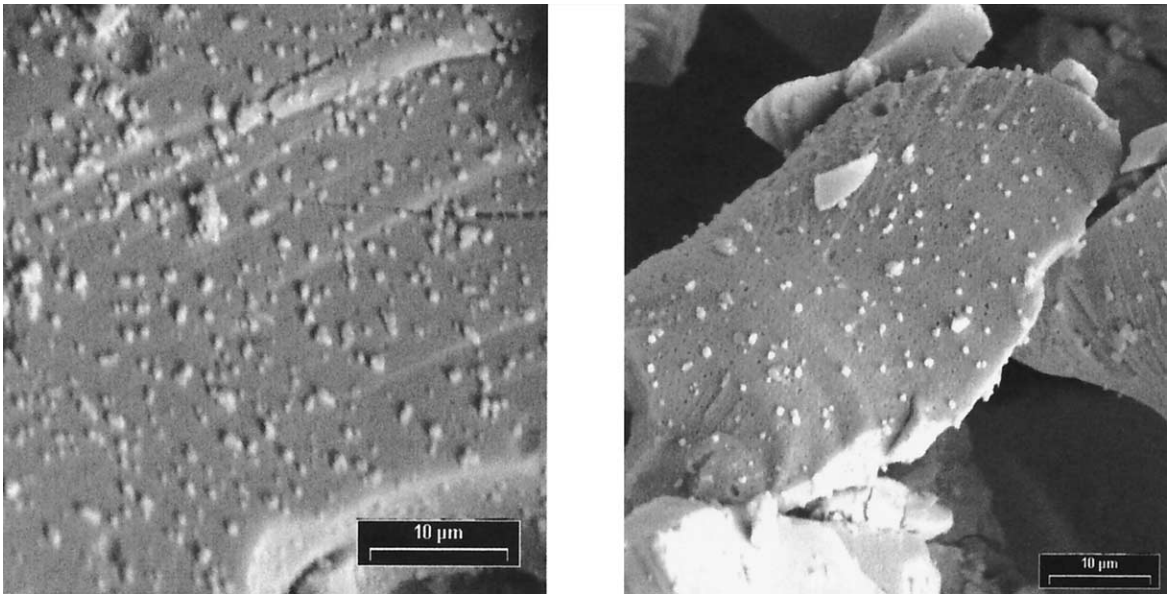


Fig. 4. SEM photomicrographs of oxidized AsS (am) with the formation of fine particles (Exp. # A).

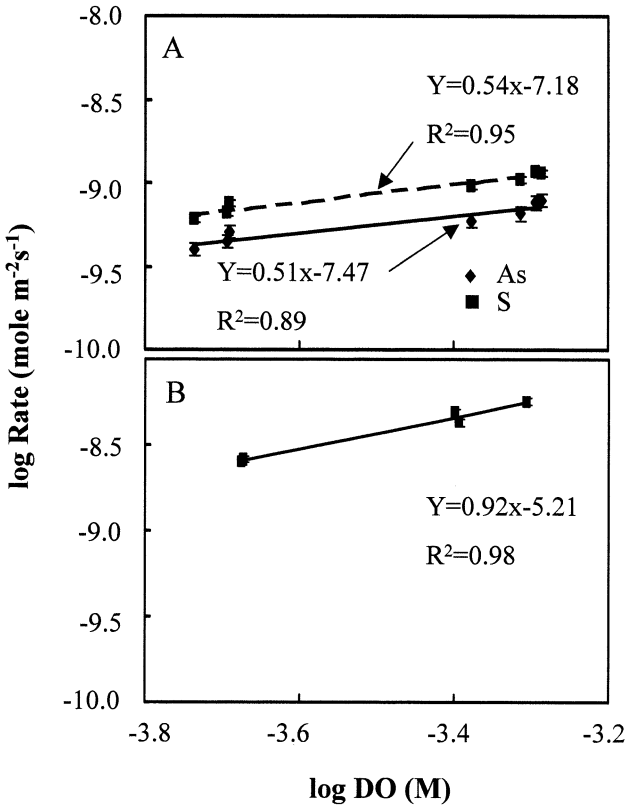


Fig. 5. The effect of dissolved oxygen concentrations on the oxidation rates of (A) realgar at pH ~8 and 25°C, and (B) AsS (am) at pH ~7.9 and 25°C.

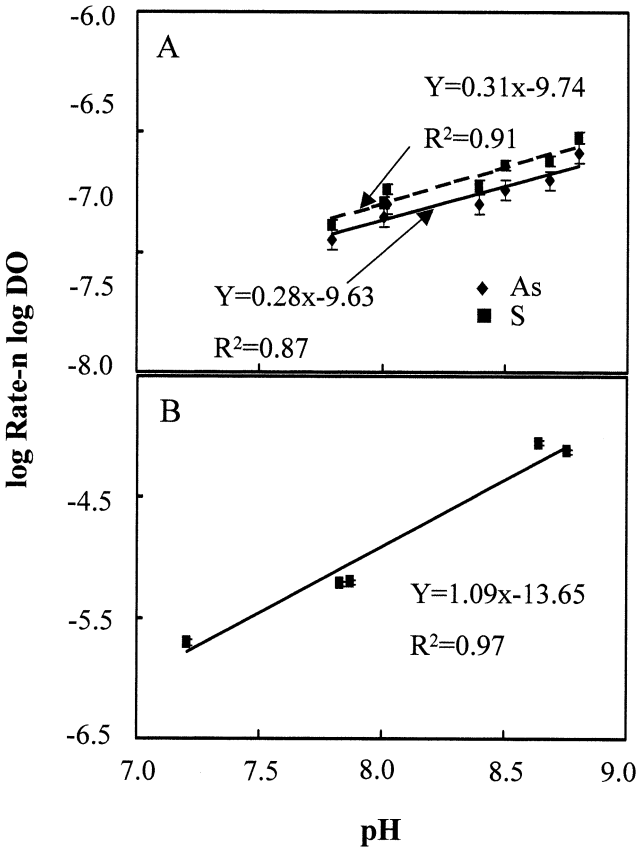


Fig. 6. The dependency of pH upon the oxidation rates at 25°C of (A) realgar oxidation, (B) AsS (am).

$$R_{(Realgar/As)} = 10^{-9.63(\pm0.41)}[DO]^{0.51(\pm0.08)}[H^+]^{-0.28(\pm0.05)} \quad (5)$$

$$R_{(Realgar/S)} = 10^{-9.74(\pm0.35)}[DO]^{0.54(\pm0.05)}[H^+]^{-0.31(\pm0.04)} \quad (6)$$

$$R_{(AsS\ (am))} = 10^{-13.65(\pm0.82)}[DO]^{0.92(\pm0.08)}[H^+]^{-1.09(\pm0.01)} \quad (7)$$

where [DO] is the dissolved oxygen content (M) and $[H^+]$ is the proton concentration (M). For all experiments, the concentrations of dissolved species in output solutions are relatively low (<0.02 mol/L). Thus, the concentration of $H^+$ is assumed to be equal to the activity of $H^+$.

### 3.3. The Effect of Temperature

The temperature (T) dependence of the rate constant (k) by the Arrhenius equation is:

$$\log k = \left(-\frac{E_a}{2.303R}\right)\left(\frac{1}{T}\right) + \log A \quad (8)$$

where $E_a$ is an activation energy of reaction, R is the gas constant, and A is a preexponential factor. Thus, a plot of log k vs. 1/T should yield a straight line with slope of $-E_a/2.303R$.

The oxidation rate of AsS (am) increases with increasing temperature (25 to 40°C) at pH ~7.7, as shown in Figure 7B (Table 3, Exp. # C, CC, D, DD, E, and EE). The Arrhenius plot of the log rate constant vs. 1000/T(K) yields the following equation:

$$\log k = -6.48(\pm0.98)(1000/T) + 7.86(\pm3.22), \quad R^2 = 0.92 \quad (9)$$

The calculated apparent activation energy using the slope of the data is 124.1 ± 18.8 kJ/mol.

The effect of temperature on realgar oxidation was determined using several experiments conducted from 25 to 40°C at pH ~8 (Table 2, Exp. # P, X, Y, YY, Z, ZZ, and ZZZ). The plot of log rate constant (k) vs. 1000/T(K) yields slopes of 3.35 ± 0.51 and 3.26 ± 0.47 for As and S, respectively (Fig. 7A). The derived slopes correspond to activation energies of 64.2 ± 9.8 and 62.2 ± 9.0 kJ/mol based on the Arrhenius equation.

### 3.4. Intermediate Sulfoxy Anions and Arsenic Species

Analysis of sulfur speciation during AsS (am) oxidation shows that sulfate ($SO_4^{2-}$), thiosulfate ($S_2O_3^{2-}$), and sulfite ($SO_3^{2-}$) are below the detection limits of ion chromatography, whereas sulfate is present in measurable amounts (10 to 35%) during realgar oxidation (Table 4). This observation indicates that aqueous sulfur species with intermediate oxidation states other than sulfite and thiosulfate occur during the oxidation of realgar and AsS (am). However, no further study was conducted to investigate the sulfur species. Arsenic speciation indicates that both As(III) and As(V) are present for most

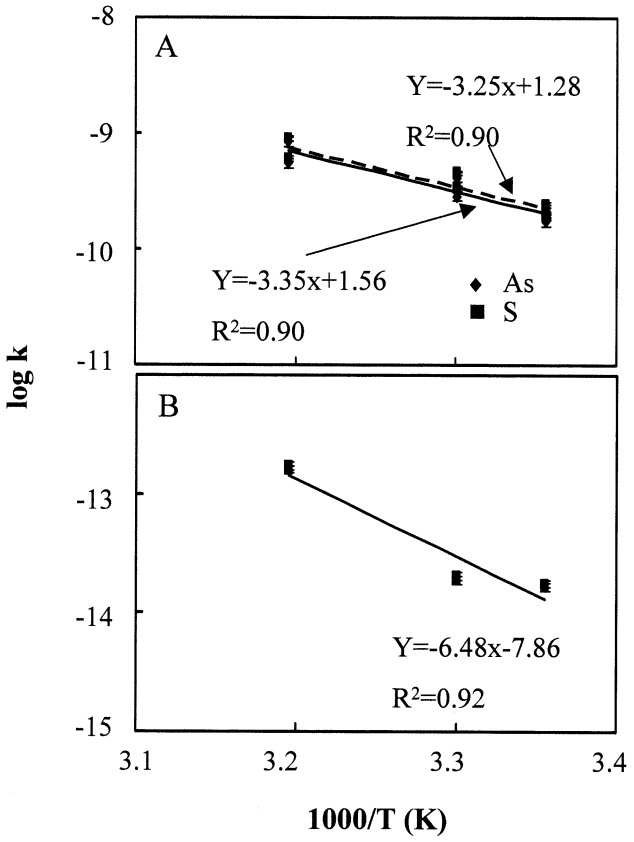


Fig. 7. Arrhenius plots for the oxidation rate constants of (A) realgar oxidation at pH ~8 and 25 to 40°C, (B) AsS (am) at pH ~7.7 and 25 to 40°C.

experiments, and that As(III) is more dominant than As(V), as shown in Tables 5 and 6.

### 3.5. Oxygen Consumption During Realgar and AsS (am) Oxidation

Dissolved oxygen consumption was calculated by determining the difference between DO concentrations in feed solutions and those at steady-state conditions. Although DO consumption may not represent the exact amounts of DO used during the oxidation reactions, these values may provide clues to mechanisms of realgar and AsS (am) oxidation. Plots of log DO consumption vs. log initial DO concentration and log oxidation rates of AsS (am) and realgar at pH ~8 and 25°C are presented in Figure 8 (Table 2, Exp. # P, S, U, V, XX, Z, ZZZ and Table 3, Exp. # C, CC, F, FF, and H). The plots show that DO consumption increases for both realgar and AsS (am) oxidation reactions at higher initial DO concentrations and as the oxidation rates increase.

Plots of log DO consumption vs. pH and log oxidation rate for both realgar and AsS (am) oxidation within the pH range of 7.2 to 8.8 at 25°C are shown in Figure 9. In both cases, DO consumption increases at higher pH along with oxidation rates. The plots of DO consumption vs. oxidation rates at various pH and DO concentrations suggest that dissolution of realgar and AsS (am) is a function of oxidation reactions at these DO and pH values.

When comparing the DO consumption of realgar to AsS(am), the amounts of DO consumed are higher for realgar where the rates of realgar oxidation are lower (Tables 2 and 3), at similar pH value and starting DO concentration (Fig. 10). This observation suggests that the oxygen consumption amounts differ with the solids. Thus, differences in DO consumption during oxidation reactions may result from different mechanisms for realgar and AsS(am) oxidation.

### 3.6. Possible Reactions During Realgar and AsS (am) Oxidation

High calculated activation energy of realgar and AsS (am) suggests that surface reaction is the dominant mechanism of oxidation. Because the oxidation state of As in the solid AsS (am) is +2 and As(II) does not exist in aqueous solution, the oxidation reaction of As(II) to As(III) should occur in the solid phase of realgar and AsS (am) before As(III) is released to the solution. Additionally, the electron configuration of As (II), [Ar] $3d^{10}4s^{2}4p^{1}$, is an unstable configuration and is more likely to release one electron to reach a stable configuration of As(III). The problem exists in explaining the surface reaction involving

Table 4. Sulfur species summary during realgar oxidation.

| Exp. # | $mS_{(T)}$ (mM) | $SO_4^{2-}$ (mM) | $SO_4^{2-}$ (%) | $S_2O_3^{2-}$ (mM) | $S_2O_3^{2-}$ (%) | $SO_3^{2-}$ (mM) | $SO_3^{2-}$ (%) | Other S (mM) | Other S (%) |
|---|---|---|---|---|---|---|---|---|---|
| Z | 0.027 | 0.005 | 19.0 | <0.003 | — | <0.003 | — | 0.022 | 81.0 |
| ZZZ | 0.024 | — | — | — | — | — | — | 0.024 | 100.0 |
| Y | 0.024 | 0.006 | 24.3 | 0.004 | 18.9 | <0.003 | — | 0.009 | 37.9 |
| X | 0.044 | 0.005 | 11.9 | <0.003 | — | <0.003 | — | 0.039 | 88.1 |
| W | 0.028 | 0.004 | 13.0 | <0.003 | — | <0.003 | — | 0.024 | 87.0 |
| V | 0.026 | 0.005 | 18.4 | <0.003 | — | <0.003 | — | 0.021 | 81.6 |
| U | 0.028 | 0.007 | 25.9 | <0.003 | — | <0.003 | — | 0.021 | 74.1 |
| T | 0.028 | 0.004 | 13.2 | <0.003 | — | <0.003 | — | 0.024 | 86.8 |
| S | 0.023 | 0.007 | 31.1 | <0.003 | — | <0.003 | — | 0.016 | 68.9 |
| ZZ | 0.028 | 0.005 | 16.7 | <0.003 | — | <0.003 | — | 0.023 | 83.3 |
| YY | 0.047 | 0.009 | 19.8 | 0.006 | 12.2 | <0.003 | — | 0.026 | 55.7 |
| XX | 0.047 | 0.005 | 10.0 | <0.003 | — | <0.003 | — | 0.042 | 90.0 |
| WW | 0.017 | 0.006 | 34.7 | <0.003 | — | <0.003 | — | 0.011 | 65.3 |
| VV | 0.023 | 0.005 | 22.2 | <0.003 | — | <0.003 | — | 0.018 | 77.8 |
| UU | 0.021 | 0.004 | 19.5 | <0.003 | — | <0.003 | — | 0.017 | 80.5 |
| P | 0.022 | 0.006 | 27.9 | <0.003 | — | <0.003 | — | 0.016 | 72.1 |

Table 5. Concentrations and percentages of arsenic species relative to total arsenic in solutions during AsS (am) oxidation.

| Exp. # | pH | mAs (mM) | As(III) (mM) | As(III) (%) | As(V) (mM) | As(V) (%) | As(III)/ As(V) |
|---|---|---|---|---|---|---|---|
| A | 8.76 | 1.40E-01 | 5.77E-02 | 41.25 | 8.23E-02 | 58.75 | 0.70 |
| AA | 8.64 | 1.24E-01 | 7.03E-02 | 56.48 | 5.42E-02 | 43.52 | 1.30 |
| B1 | 7.21 | 6.80E-03 | 4.67E-03 | 68.63 | 2.13E-03 | 31.37 | 2.19 |
| C | 7.89 | 1.94E-02 | 1.35E-02 | 69.69 | 5.87E-03 | 30.31 | 2.30 |
| CC | 7.87 | 1.94E-02 | 1.39E-02 | 71.5 | 5.53E-03 | 28.5 | 2.51 |
| D | 7.82 | 1.88E-02 | 1.50E-02 | 79.57 | 3.84E-03 | 20.43 | 3.91 |
| DD | 7.82 | 1.93E-02 | 1.29E-02 | 66.64 | 6.45E-03 | 33.36 | 2.00 |
| E | 7.59 | 5.10E-02 | 2.66E-02 | 52.21 | 2.44E-02 | 47.79 | 1.09 |
| EE | 7.56 | 5.11E-02 | 2.66E-02 | 52.08 | 2.45E-02 | 47.92 | 1.09 |
| F | 7.73 | 4.99E-02 | 2.77E-02 | 55.41 | 2.23E-02 | 44.59 | 1.24 |
| FF | 7.93 | 3.00E-02 | 1.64E-02 | 54.54 | 1.36E-02 | 45.46 | 1.21 |
| H | 8.01 | 3.01E-02 | 2.09E-02 | 69.3 | 9.25E-03 | 30.7 | 2.26 |

realgar and AsS (am) because the reaction mechanisms for changing the oxidation state from +2 to +3 are not known. As(II) may be oxidized to As(III) on the solid surface by the following reaction:

$$\equiv As(II) + 0.25\,O_2 + H^+ \rightarrow \equiv As(III) + 0.5\,H_2O \quad (10)$$

where ≡ is the surface reaction notation. This reaction shows that a proton and oxygen are necessary for oxidation of As(II) to As(III), and that the proton is more important than oxygen based on the stoichiometric value from reaction (10). Proton concentration increases with decreasing pH values, thus at lower pH values, the oxidation of As(II) to As(III) on the solid AsS (am) is favored. Arsenic(III) may then be released to the aqueous solution as $H_3AsO_3$ by the following reaction:

$$\equiv As(III) + 3H_2O \rightarrow H_3AsO_{3(aq)} + 3\,H^+ \quad (11)$$

If reaction (10) is kinetically faster than reaction (11), then an increase in pH and decrease in DO would be observed as is the case in all realgar oxidation experiments. However, decreases in both pH and DO were observed for all AsS (am) experiments. This observation may be explained as the overall hydrolysis reaction of As(II) oxidation to As(III), $H_3AsO_3$, and may be written as:

$$\equiv As(II) + 0.25\,O_2 + 2.5\,H_2O \rightarrow H_3AsO_{3(aq)} + 2\,H^+ \quad (12)$$

Based on the above reaction, a decrease in both pH and DO should be observed.

When dissolved oxygen is the primary oxidant, the realgar and AsS (am) oxidation reaction may be written as follows:

$$AsS + 2.25O_2 + 2.5H_2O \rightarrow H_3AsO_3 + SO_4^{2-} + 2H^+ \quad (13)$$

$$H_3AsO_3 + 0.5O_2 \rightarrow HAsO_4^{2-} + 2H^+ \quad (14)$$

or

$$H_3AsO_3 + 0.5O_2 \rightarrow H_2AsO_4^- + H^+ \quad (15)$$

However, the above oxidation pathways involve intermediate steps and the kinetics of each reaction may be very different. In reaction (13), eight electrons per mole of sulfur are transferred during the oxidation of realgar to sulfate. The sulfur speciation results show that aqueous sulfur species with intermediate oxidation states form during the realgar and AsS (am) oxidation experiments. Partial oxidation of As(III) to As(V) is also observed. Because it is unlikely for eight electrons to be transferred during one redox reaction, intermediate oxidation states of sulfur must be involved. This study shows that the oxidation

Table 6. Arsenic species summary during realgar oxidation.

| Exp. # | pH | mAs (mM) | As(III) (mM) | As(III) (%) | As(V) (mM) | As(V) (%) | As(III)/ As(V) |
|---|---|---|---|---|---|---|---|
| Z | 8.02 | 1.84E-02 | 1.31E-02 | 71.1 | 5.32E-03 | 28.90 | 2.46 |
| ZZZ | 8.01 | 1.61E-02 | 1.32E-02 | 82.2 | 2.87E-03 | 17.84 | 4.60 |
| Y | 8.00 | 1.61E-02 | 1.33E-02 | 83.0 | 2.73E-03 | 17.01 | 4.88 |
| X | 8.13 | 2.98E-02 | 2.09E-02 | 70.2 | 8.88E-03 | 29.84 | 2.35 |
| W | 8.68 | 1.80E-02 | 1.40E-02 | 77.7 | 4.01E-03 | 22.25 | 3.49 |
| V | 8.00 | 1.75E-02 | 6.02E-03 | 34.4 | 1.15E-02 | 65.55 | 0.53 |
| U | 8.05 | 1.83E-02 | 7.00E-03 | 38.3 | 1.13E-02 | 61.68 | 0.62 |
| T | 8.80 | 1.84E-02 | 1.08E-02 | 58.8 | 7.56E-03 | 41.18 | 1.43 |
| S | 8.02 | 1.44E-02 | 6.79E-03 | 47.0 | 7.65E-03 | 52.97 | 0.89 |
| ZZ | 8.04 | 1.80E-02 | 1.20E-02 | 66.7 | 6.00E-03 | 33.33 | 2.00 |
| YY | 7.73 | 3.38E-02 | 2.65E-02 | 78.3 | 7.35E-03 | 21.73 | 3.60 |
| XX | 8.02 | 2.92E-02 | 1.25E-02 | 42.6 | 1.68E-02 | 57.35 | 0.74 |
| WW | 7.80 | 1.11E-02 | 6.12E-03 | 55.0 | 5.01E-03 | 44.98 | 1.22 |
| VV | 8.40 | 1.51E-02 | 8.20E-03 | 54.2 | 6.93E-03 | 45.81 | 1.18 |
| UU | 8.78 | 1.30E-02 | 8.33E-03 | 64.1 | 4.67E-03 | 35.90 | 1.79 |
| P | 8.10 | 1.47E-02 | 8.47E-03 | 57.7 | 6.20E-03 | 42.27 | 1.37 |

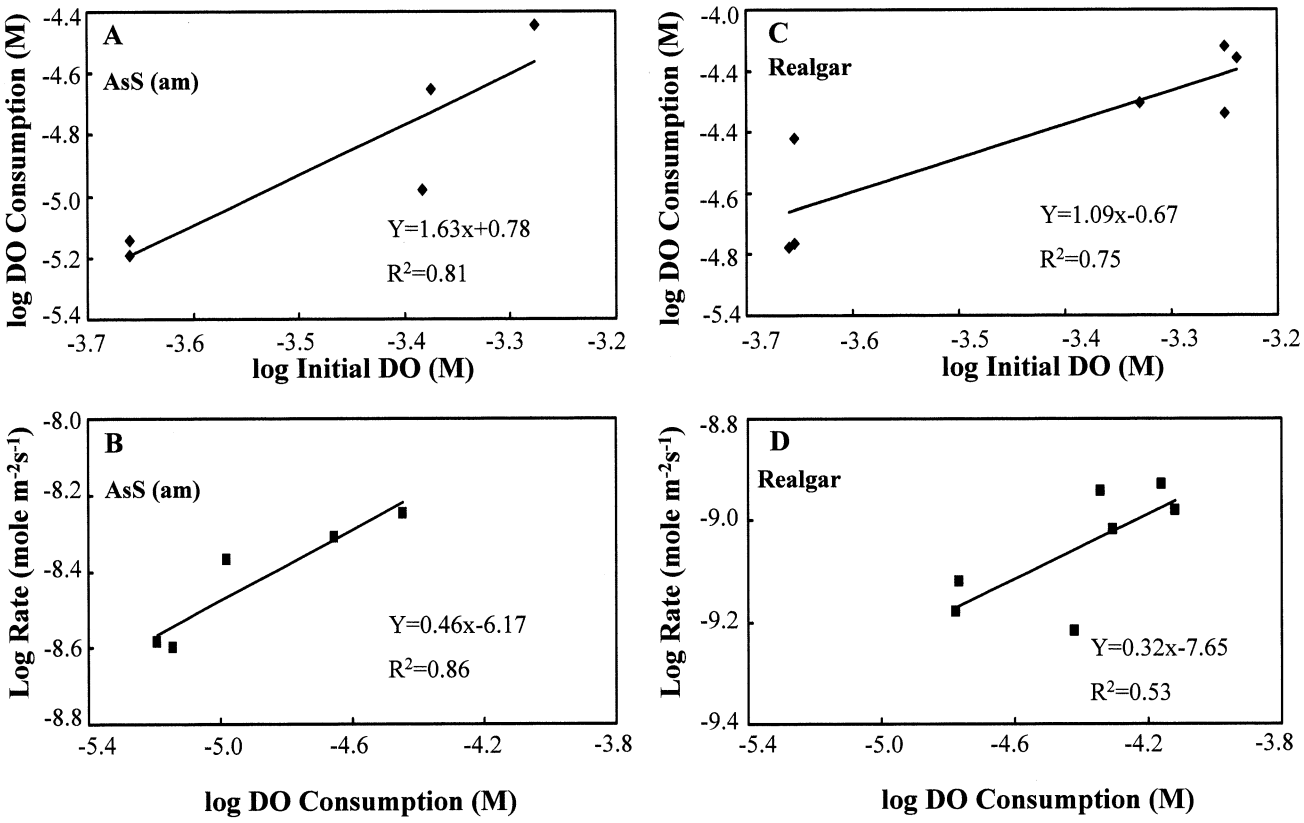


Fig. 8. The initial dissolved oxygen concentrations and oxidation rates vs. the amounts of dissolved oxygen consumption during (A, B) AsS (am) and (C, D) realgar oxidation at 25°C and pH ~8.

of realgar and AsS (am) cannot be represented by a simple elementary reaction. Despite the fact that the complex reaction mechanisms cannot be described by our present state of research, we hope that this study will provide the basis for future research in arsenic sulfide oxidation.

### 3.7. Mechanistic Implications of Rate Laws

Square-root dependencies on heterogeneous rate laws generally indicate that the mechanism involves dissociation of a species adsorbed on the surface (Lasaga, 1981).

The dependency factor on oxygen molarity for realgar oxidation by dissolved oxygen is close to 0.5, whereas AsS (am) shows higher DO dependency (~1). These factors suggest that the realgar oxidation mechanisms in the near neutral to alkaline solutions involve dissociation of oxygen adsorbed on arsenic sulfide solid surfaces, if desorption of products is not rate-limiting. Pyrite oxidation also has an oxygen reaction order of 0.5 (McKibben and Barnes, 1986; Williamson and Rimstidt, 1994). Pyrite oxidation is an electrochemical process where the overall oxidation process of pyrite is the sum of the cathodic and anodic reactions occurring at the surface involving nonsite-specific, multiple-layer adsorption of the oxidant (Lowson, 1982; Williamson and Rimstidt, 1994). The rate of pyrite destruction is positively correlated with the concentration of the oxidant, indicating that electron transfer from the mineral to the aqueous oxidant is rate-limiting (Williamson and Rimstidt, 1994). The similar dependency factor upon oxygen during realgar oxidation indicates that the transfer of electrons from the mineral to $O_2$ may be similar to the rate-limiting step during pyrite oxidation.

### 3.8. Natural Realgar vs. AsS (am) Oxidation Rates

Dissolved oxygen and pH influence the oxidation rates of both natural realgar and AsS (am). Comparison of both natural realgar and AsS (am) oxidation rates as a function of pH, DO contents, and temperature is illustrated in Figure 11. The amorphous AsS oxidation rates were always faster than natural realgar by a factor ranging from 2 to 38 under similar experimental conditions. The oxidation of realgar involves the destruction of the crystallographic framework at the water–solid interface, whereas AsS (am) does not have any crystal structure to dissolve. Thus, the As and S release rates from AsS (am) are faster than those from realgar.

The AsS (am) oxidation shows higher dependency on pH and DO than that of realgar. The activation energy of AsS (am) at pH ~8 and a temperature range of 25 to 40°C is almost twice as large as that of realgar. This difference in activation energy may be due to different reactions, bond strength, and bond energy between natural realgar and AsS (am). The dominant reaction products during realgar and AsS (am) oxidation are similar and consist of As (III), As(V), and aqueous sulfur species with intermediate oxidation states. Although AsS (am) oxidation shows a stoichiometric ratio of As/S, oxidation of realgar is nonstoichiometric in all experiments due to possible

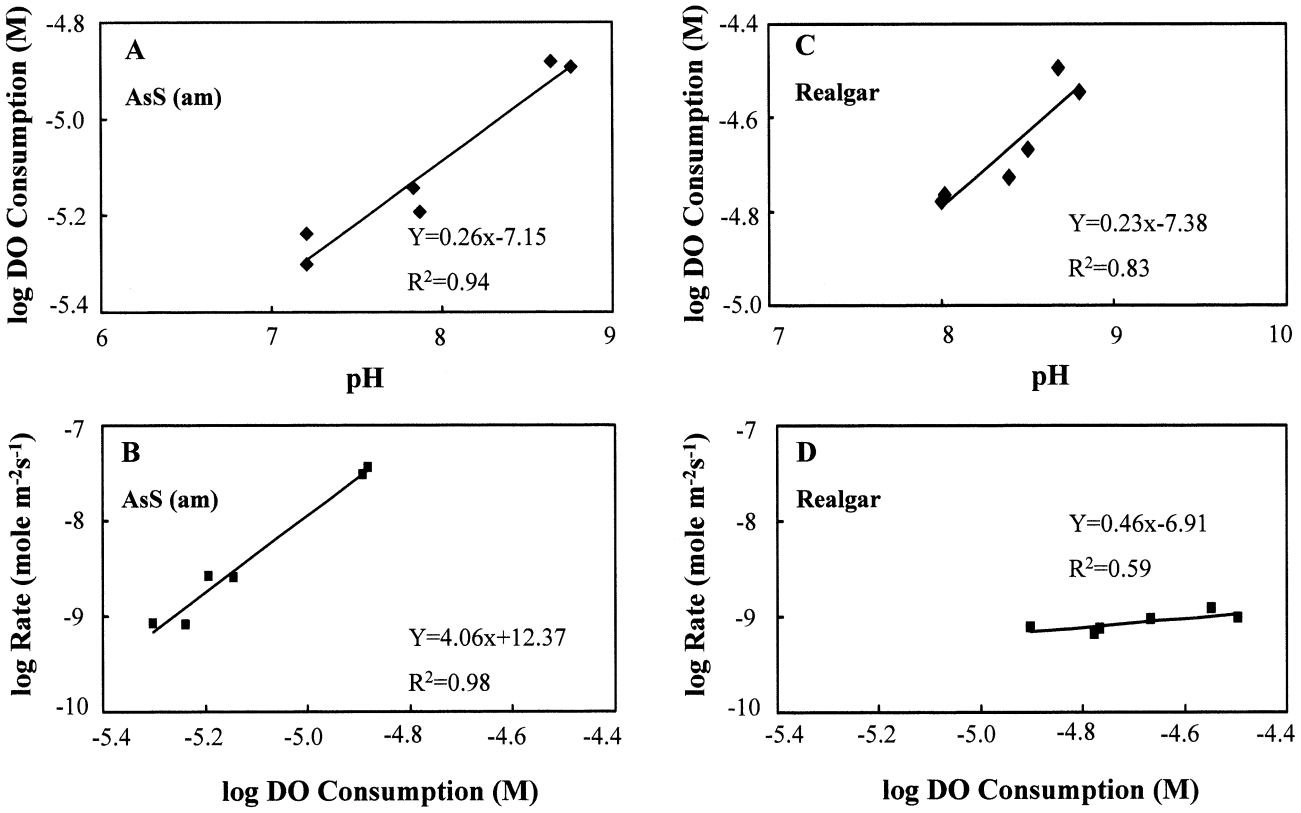


Fig. 9. The dissolved oxygen consumption vs. pH and oxidation rates of (A, B) AsS (am) and (C, D) realgar at 25°C.

precipitation of secondary phases, the presence of impure mineral phases, oxidative leaching, or a lower diffusion rate of As from realgar lattice to surfaces during steady-state conditions. Although the oxidation rates of AsS (am) may not represent those of realgar and the occurrence of AsS (am) in the natural environment is not widespread, knowledge of the fundamental controls on oxidation of AsS (am) may be useful in understanding realgar oxidation. Moreover, natural realgar is rarely found as a pure mineral in the natural environment, and the presence of solid solution associated with realgar may have an effect on realgar oxidation, causing problems in quantifying rates and understanding the oxidation mechanisms.


Fig. 10. Comparison of dissolved oxygen consumption between realgar and AsS (am) oxidation at pH ~8 and 25°C.

## 4. CONCLUSIONS

The factors affecting the realgar and AsS (am) oxidation kinetics, including pH, DO, and temperature, were assessed using mixed flow reactors. The main observations are as follows:

A good linear relationship is observed between log oxidation rates and pH/DO contents. The DO-dependence factors of realgar oxidation rates are 0.51 ± 0.08 and 0.54 ± 0.05 at 25°C for As and S, respectively. The reaction orders on pH are 0.28 ± 0.05 and 0.31 ± 0.04 for As and S, respectively. The oxidation rates of AsS (am) are significantly affected by DO and pH. The reaction orders for AsS (am) upon DO and pH are 0.92 and 1.09 for DO and pH, respectively.

The calculated activation energy at approximately pH ~7.7 for AsS (am) oxidation by oxygen over a temperature range from 25 to 40°C is 124.1 kJ/mol and those for realgar oxidation at pH ~8 are 64.2 ± 9.8 and 62.2 ± 9.0 kJ/mol for As and S, respectively. Large differences in activation energy for natural realgar and AsS (am) oxidation may be caused by different reactions, bond strength, or bond energy involved during oxidation reactions.

The ratios of As/S are close to stoichiometric for most AsS (am) experiments, except for experiments at pH ~8.8. In these

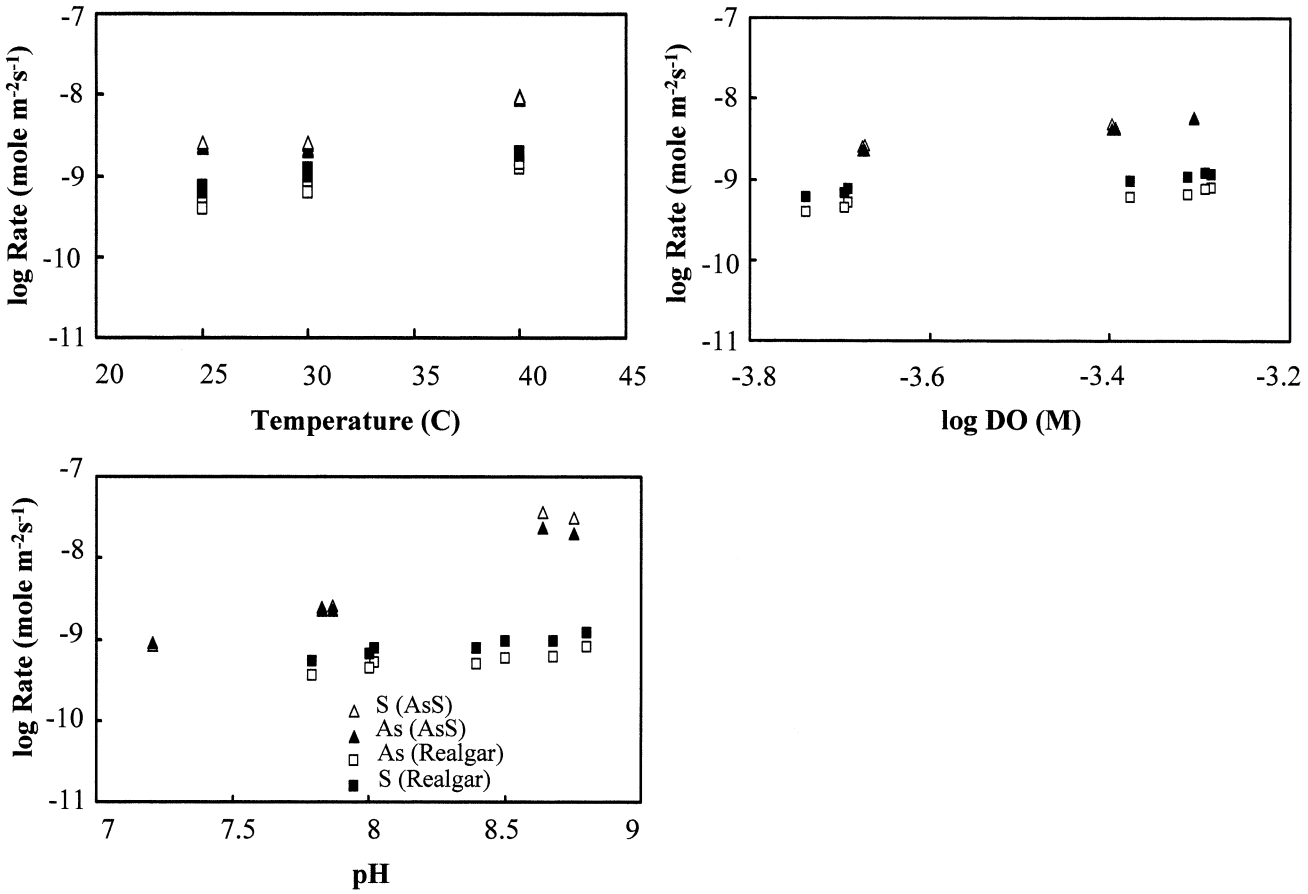


Fig. 11. Comparison of realgar and AsS (am) oxidation rates as a function of pH, DO, and temperature.

experiments, nonstoichiometric ratios may be explained by secondary precipitation on AsS (am) surfaces. The realgar oxidation was nonstoichiometric, and the preferential release of S relative to As for all experiments during steady-state conditions was observed. This observation could be caused by low diffusion rates of As from the realgar lattice to the near-surface region during steady-state conditions. Moreover, the presence of impurities within the realgar may also cause the observed nonstoichiometric dissolution. XRD and SEM results suggest that no secondary phases are detectable, and these findings were corroborated with solubility calculations.

The DO consumption increases as the oxidation rates of realgar and AsS (am) increase. This observation suggests that dissolution of realgar and AsS (am) is a function of oxidation reactions within the considered experimental conditions.

The amounts of DO consumption for realgar are higher than those for AsS (am) at pH ~8 where the rates of realgar oxidation are lower than those of AsS (am). This observation suggests that oxidation paths, reaction steps, and reaction products of realgar oxidation may not be the same as those of AsS (am) oxidation, resulting in different amounts of DO consumption.

As(III) and As(V) are present during both realgar and AsS (am) oxidation. Aqueous sulfur species other than sulfate, sulfite, and thiosulfate are the dominant product during AsS (am) oxidation and may involve intermediate sulfur oxidation states.

Oxidation rates of realgar are always slower that those of AsS (am) by a factor ranging from 2 to 38 within similar experimental conditions. The destruction of the crystal framework may account for the fact that realgar oxidation is slower than that of AsS (am).

*Acknowledgments*—The authors gratefully acknowledge partial support from Placer Dome, Inc. for this research. Valuable comments from J. D. Rimstidt, R. V. Nicholson, S. J. Traina, and one anonymous reviewer contributed to the final product. The authors would like to thank Dr. Mae Gustin for the use of analytical instruments in her laboratory.

## REFERENCES

Barrante J. R. (1998) *Applied Mathematics for Physical Chemistry*. Prentice-Hall. 179–191.

Brunauer S., Emmet P. S., and Teller E. (1938) Adsorption of gases in multimolecular layers. *J. Am. Chem. Soc.* **60,** 309–319.

Buckley A. N. and Woods R. (1987) The surface oxidation of pyrite. *Appl. Surf. Sci.* **27,** 437–452.

Craig J. R. and Vaughan D. J. (1981) *Ore Microscopy and Ore Petrography*, John Wiley & Sons, New York. 406 p.

Douglass D. L., Shing C., and Wang G. (1992) The light-induced alteration of realgar to pararealgar. *Am. Mineral.* **77,** 1266–1274.

Ehrlich H. L. (1963) Bacterial action on orpiment. *Econ. Geol.* **58,** 991–994.

Forneris R. (1969) The infrared and Raman spectra of realgar and orpiment. *Am. Mineral.* **54,** 1062–1074.

Hugi M. (1988) Die Quarze der Mineraliengrube Lengenbach. (Binntal, VS) and ihr Einsclusse. Ph.D. Dissertation, University of Bern, Switzerland (unpub.).

Lasaga A. C. (1981) Rate laws of chemical reactions. In *Kinetics of Geochemical Processes* (eds. A. C. Lasaga and R. J. Kirkpatrick). Min. Soc. of America, *Reviews in Mineralogy* **8,** 1–68.

Lazaro I., Gonzalez I., Cruz R., and Monroy M. G. (1997) Electrochemical study of orpiment ($As_2S_3$) and realgar ($As_2S_2$) in acidic medium. *J. Electrochem. Soc.* **144,** 4128–4132.

Lengke M. F. (2001) Arsenic sulfide oxidation kinetics. Ph.D. dissertation, University of Nevada, Reno, Nevada (unpub.), 204 pp.

Lengke M. F. and Tempel R. N. (2001) Kinetic rates of amorphous $As_2S_3$ oxidation at 25 to 40°C and initial pH of 7.3 to 9.4. *Geochim. Cosmochim. Acta* **65,** 2241–2255.

Lengke M. F. and Tempel R. N. (2002) Reaction rates of natural orpiment oxidation at 25 40°C and pH 6.8 to 8.2 and comparison with amorphous $As_2S_3$ oxidation. *Geochim. Cosmochim. Acta* **66,** 3281–3291.

Levenspiel O. (1972) *Chemical Reaction Engineering*. John Wiley & Sons, New York. 578 p.

Lowson R. T. (1982) Aqueous pyrite oxidation by molecular oxygen. *Chem. Rev.* **82,** 461–497.

McKibben M. A. and Barnes H. L. (1986) Oxidation of pyrite in low temperature acidic solutions: Rate laws and surface textures. *Geochim. Cosmochim. Acta* **50,** 1509–1520.

Nesbitt H. W., Muir I. J., and Pratt A. R. (1995) Oxidation of arsenopyrite by air and air-saturated, distilled water, and implications for mechanism of oxidation. *Geochim. Cosmochim. Acta* **59,** 1773–1786.

Nicholson R. V. and Scharer J. M. (1994) Laboratory studies of pyrrhotite oxidation kinetics. In *Environmental Geochemistry of Sulfide Oxidation* (eds. C. N. Alpers and D. W. Blowes), pp. 14–30. American Chemical Society.

Parkhurst D. L. (1995) User's guide to PHREEQC—A computer program for speciation, reaction-path, advective-transport, and inverse geochemical calculations. U. S. G. S Water-Resources Investigations Report 95-4227.

Radtke A. S. (1981) Geology of the Carlin gold deposit, Nevada. U. S. Geological Survey Open-File Report 81-97.

Rimstidt J. D., Chermak J. A., and Gagen P. M. (1994) Rates of reaction of galena, sphalerite, chalcopyrite, and arsenopyrite with Fe(III) in acidic solutions. In *Environmental Geochemistry of Sulfide Oxidation* (eds. C. N. Alpers and D. W. Blowes), pp. 2–13. American Chemical Society.

Smith A. H., Hopenhayn-Rich C., Bates M. N., Goeden H. M., Herz-Picciotto I., Duggan H. M., Wood R., and Kosnett M. J. (1992) Cancer risks from arsenic in drinking water. *Env. Health Perspec.* **97,** 259–267.

Welch A. H., Lico M. S., and Hughes L. (1988) Arsenic in ground water of the Western United States. *Ground Water* **26,** 333–347.

Williamson M. A. and Rimstidt J. D. (1994) The kinetics and electrochemical rate-determining step of aqueous pyrite oxidation. *Geochim. Cosmochim. Acta* **58,** 5443–5454.